GEOMETRIC OPTIMIZATION OF PLANAR 3-*RPR* PARALLEL MECHANISMS

Qimi Jiang[1], Clément M. Gosselin[2]

[1]Département de Génie Mécanique, Université Laval, qimi.jiang.1@ulaval.ca
[2]Département de Génie Mécanique, Université Laval, gosselin@gmc.ulaval.ca

Received June 2007, Accepted October 2007
No. 07-CSME-56, E.I.C. Accession 3025

ABSTRACT

To pursue the maximal singularity-free workspace of parallel mechanisms is a very important concern for robot designers. This paper focuses on the case of planar 3-*RPR* parallel mechanisms. First, a relatively simple singularity equation of any point on the platform is derived. The obtained singularity equation shows that the singularity locus of any point on the platform is a circle of the same size, as long as the base and the platform are similar triangles. Furthermore, the three centres of the workspace circles lie exactly on the singularity circle. With these useful observations, the singularity-free workspace as well as the maximal leg length ranges can be determined. For a base of unit area, it is found that robots with equilateral triangle base and platform can obtain the maximal singularity-free workspace. Three case studies demonstrate this observation. Finally, a procedure for this kind of robot geometric design is provided.

Keywords: Planar 3-*RPR* Parallel Mechanisms, Workspace Circle, Singularity-Free Workspace, Geometric Optimization.

OPTIMISATION GÉOMÉTRIQUE DES MÉCANISMES PARALLÈLES PLANS DE TYPE 3-*RPR*

RÉSUMÉ

Déterminer l'espace de travail maximal sans singularité des mécanismes parallèles est un souci très important pour les concepteurs mécaniques de robots. Cet article se concentre sur le cas des mécanismes parallèles plans de type 3-*RPR*. Premièrement, une équation simple donnant l'ensemble des lieux de singularité du mécanisme étudié est présentée. Cette équation de singularité obtenue démontre que le lieu de singularité de chaque point sur la plate-forme est un cercle de même dimension, et ce aussi longtemps que la base et la plate-forme sont des triangles semblables. En outre, les trois centres des cercles déterminant l'espace de travail sont situés directement sur les cercles de singularité. Avec ces observations utiles, l'espace de travail libre de singularité ainsi que la longueur maximale des membrures peuvent être déterminés. Pour une base d'aire unitaire, il est montré qu'un mécanisme ayant à la fois la plate-forme et la base de la forme d'un triangle équilatéral possède l'espace de travail sans singularité maximal. Trois cas présentés démontreront cette observation. Finalement, une procédure de conception pour des robots de cette géométrie sera donnée.

Mots clé: Mécanismes Parallèles Plans 3-*RPR*, Cercle de Zone de Travail, Zone de Travail Libre de Singularité, Optimisation Géométrique.

1 INTRODUCTION

Parallel mechanisms have many advantages over serial mechanisms in load-carrying capacity, stability, etc. However, the closed-loop nature of their architecture limits the motion of the platform and creates complex kinematic singularities inside the workspace. Hence, to pursue the maximal singularity-free workspace of parallel mechanisms is highly desirable for robot designers.

Several researchers addressed the issue of avoiding singularities inside the workspace of a parallel mechanism. Merlet [1] presented a fast algorithm for solving the problem of trajectory validation for a 6-DOF parallel mechanism with respect to its workspace. Bhattacharya et al. [2] proposed an exact method and an approximate method to determine a path which can avoid singularities and remain close to a prescribed path. Dash et al. [3] presented a numerical technique for path planning inside the workspace of parallel mechanisms avoiding singularities.

Three types of singularities were defined by Gosselin and Angeles [4; 5]. They are the inverse kinematic singularity, the direct kinematic singularity and the architecture singularity. Each of them has a different physical interpretation. Later, another type of singularity referred to as combined singularity or constraint singularity was identified by Zlatanov, et al. [6]. Among all these types of singularities, the direct kinematic singularity is the main concern for robot designers. It corresponds to configurations in which the stiffness of the mechanism is locally lost. This type of singularity is also called RO (Redundant Output) in Zlatanov et al. [7]. This paper focuses on analyzing this type of singularity of 3-*RPR* parallel mechanisms, which have been studied by several researchers (see for instance ([8]–[18])). However, this paper will propose a new approach to obtain the maximal singularity-free workspace by optimizing the geometric parameters.

2 SINGULARITY ANALYSIS

As shown in Fig.1, a planar 3-*RPR* parallel mechanism with actuated prismatic joints consists of a fixed triangle base $\triangle B_1B_2B_3$ and a mobile triangle platform $\triangle P_1P_2P_3$. B_i and P_i are connected via the actuated prismatic joint of variable length $\rho_i (i = 1, 2, 3)$. Passive revolute joints are located at B_i and P_i, and the mechanism has 3 DOFs. The moving platform can translate in the xy plane and rotate with respect to an axis perpendicular to the xy plane.

2.1 Singularity Equation

To derive the singularity equation, two coordinate systems are defined as shown in Fig.1. A reference frame Oxy is attached to the base by selecting B_1 as the origin O and B_1B_2 as the x axis. The mobile frame $O'x'y'$ is attached to the platform by selecting P_1 as the origin O' and P_1P_2 as the x' axis. The position of B_i in the fixed frame Oxy is denoted by vector $\mathbf{b}_i = [x_{bi}, y_{bi}]^T (i = 1, 2, 3)$ and the position of P_i in the mobile frame $O'x'y'$ is denoted by vector $\mathbf{p}'_i = [x'_{pi}, y'_{pi}]^T (i = 1, 2, 3)$. $\mathbf{b}_i$ and $\mathbf{p}'_i$ are constant vectors in their respective frames.

Let vector $\mathbf{p}_r = [x_r, y_r]^T$ denote the position of the origin O' of the mobile frame in the fixed frame and $\mathbf{Q}$ be the rotation matrix representing the rotation of the platform from frame Oxy to frame $O'x'y'$ with

$$\mathbf{Q} = \begin{bmatrix} \cos\phi & -\sin\phi \\ \sin\phi & \cos\phi \end{bmatrix} \tag{1}$$

If the position of the considered point P of the platform in the fixed and mobile frames are respectively $\mathbf{p} = [x, y]^T$ and $\mathbf{p}' = [x_p, y_p]^T$, then

$$\mathbf{p} = \mathbf{p}_r + \mathbf{Q}\mathbf{p}' \tag{2}$$

or

$$\mathbf{p}_r = \mathbf{p} - \mathbf{Q}\mathbf{p}' \tag{3}$$

So, the position of $P_i (i = 1, 2, 3)$ in the fixed frame can be expressed as

$$\mathbf{p}_i = \mathbf{p}_r + \mathbf{Q}\mathbf{p}'_i = \mathbf{p} + \mathbf{Q}(\mathbf{p}'_i - \mathbf{p}') \tag{4}$$

The length of leg i is the distance between B_i and P_i. Hence

$$\rho_i^2 = (\mathbf{p}_i - \mathbf{b}_i)^T(\mathbf{p}_i - \mathbf{b}_i) \tag{5}$$

Differentiating eq.(5) with respect to time, one obtains

$$\mathbf{A}\mathbf{v} = \mathbf{D}\dot{\boldsymbol{\rho}} \tag{6}$$

where $\dot{\boldsymbol{\rho}} = [\dot{\rho}_1, \dot{\rho}_2, \dot{\rho}_3]^T$ denotes the actuator velocities and $\mathbf{v} = [\dot{x}, \dot{y}, \dot{\phi}]^T$ the Cartesian velocity vector of the platform. $\mathbf{A}$ and $\mathbf{D}$ are two Jacobian matrices.

Referring to Fig.1, suppose, without loss of generality, that the coordinates of B_i in the fixed frame Oxy are actually B_1(0,0), $B_2(t_1,0)$ and $B_3(t_2, t_3)$ and the coordinates of P_i in the mobile frame $O'x'y'$ are P'_1(0,0), $P'_2(t_4, 0)$ and $P'_3(t_5, t_6)$. The condition for the direct kinematic singularity is $\det(\mathbf{A}) = 0$. From this and considering the above coordinates of B_i and P_i $(i = 1, 2, 3)$, the singularity equation can be obtained as follows:

$$G_1x^2 + G_2y^2 + G_3xy + G_4x + G_5y + G_6 = 0 \tag{7}$$

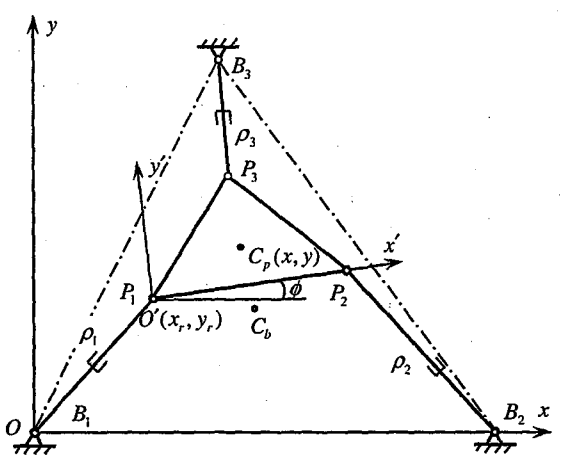

Figure 1: Planar 3-*RPR* parallel mechanism.

where

$$\begin{cases} G_1 = g_1 \sin\phi \\ G_2 = g_2 \sin\phi + g_3 \cos\phi \\ G_3 = -g_3 \sin\phi + g_4 \cos\phi \\ G_4 = g_5 \sin^2\phi + g_6 \cos^2\phi + g_7 \sin\phi\cos\phi + g_8 \sin\phi \\ G_5 = g_9 \sin^2\phi + g_{10} \cos^2\phi + g_{11} \sin\phi\cos\phi + g_{12} \sin\phi + g_{13} \cos\phi \\ G_6 = g_{14} \sin\phi + g_{15} \cos\phi + g_{16} \sin^2\phi + g_{17} \cos^2\phi + g_{18} \sin\phi\cos\phi \end{cases} \tag{8}$$

and

$$\begin{cases} g_1 = -t_3t_4 \qquad g_2 = -t_1t_6 \\ g_3 = t_1t_5 - t_2t_4 \qquad g_4 = t_3t_4 - t_1t_6 \\ g_5 = (t_2 - t_1)t_4t_5 + (t_1t_5 - t_2t_4)x_p + t_3t_4(t_6 - 2y_p) \\ g_6 = (t_1t_6 - t_3t_4)y_p \\ g_7 = t_4(t_2t_6 - t_1t_6 - t_3t_5) + (t_1t_6 + t_3t_4)x_p + (t_1t_5 - t_2t_4)y_p) \\ g_8 = t_1t_3t_4 \\ g_9 = t_1t_6(2x_p - t_4) + (t_2t_4 - t_1t_5)y_p \\ g_{10} = t_4(t_3t_5 - t_2t_6) + (t_1t_6 - t_3t_4)x_p + 2(t_2t_4 - t_1t_5)y_p \\ g_{11} = t_4(t_1t_5 - t_2t_5 - t_3t_6) + (t_2t_4 - t_1t_5)x_p + (t_1t_6 + t_3t_4)y_p \\ g_{12} = t_1(t_2t_5 - t_2t_4 + t_3t_6) \\ g_{13} = t_1(t_2t_6 - t_3t_5) \\ g_{14} = t_1t_6x_p(t_4 - x_p) + (t_1t_5 - t_2t_4)x_py_p + (t_2t_5 + t_3t_6 - t_1t_5 - t_3y_p)t_4y_p \\ g_{15} = (t_3t_4 - t_1t_6)x_py_p + (t_2t_6 - t_3t_5)t_4y_p + (t_1t_5 - t_2t_4)y_p^2 \\ g_{16} = t_1[(t_2t_4 - t_2t_5 - t_3t_6)x_p + t_3t_4y_p] \\ g_{17} = (t_3t_5 - t_2t_6)t_1y_p \\ g_{18} = (t_3t_5 - t_2t_6 - t_3t_4)t_1x_p + (t_2t_4 - t_2t_5 - t_3t_6)t_1y_p \end{cases} \tag{9}$$

If P_1 is taken as the considered point P, eq.(7) takes exactly the form given in [10].

2.2 Singularity Locus

In general, the singularity locus for a given orientation can be a hyperbola or a parabola or an ellipse [10]. Ellipses may degenerate into circles. By observation of eqs.(7)–(9), it is not difficult to find that if $t_4/t_1 = t_5/t_2 = t_6/t_3 = k$ (k is the size ratio between the platform and the base), then $g_3 \equiv g_4 \equiv 0$. As a result, $G_1 \equiv G_2$ and $G_3 \equiv 0$. In this case, the base and the platform are similar triangles, and the singularity locus expressed by eq.(7) is a circle [11]. The centre $C(x_c, y_c)$ and radius R of the singularity circle can be given as follows:

$$\begin{cases} x_c = \{[k(t_2^2 - t_1t_2 + t_3^2) - 2t_3y_p]\sin\phi + (2x_p - kt_1)t_3\cos\phi + t_1t_3\}/(2t_3) \\ y_c = \{(2x_p - kt_1)t_3\sin\phi + [k(t_1t_2 - t_2^2 - t_3^2) + 2t_3y_p]\cos\phi + t_2^2 - t_1t_2 + t_3^2\}/(2t_3) \\ R = \sqrt{[(t_1 - t_2)^2 + t_3^2](t_2^2 + t_3^2)(k^2 - 2k\cos\phi + 1)}/(2t_3) \end{cases} \tag{10}$$

Eq.(10) shows that for a given orientation $\phi \neq i\pi (i = 0, 1)$, only the centre of the singularity circle depends on the position of the considered point P. But the radius does not. When $\phi = i\pi (i = 0, 1)$, the whole plane becomes singular. Fig.2 shows the evolution of the radius R of the singularity circle with respect to the size ratio k and the orientation angle ϕ.

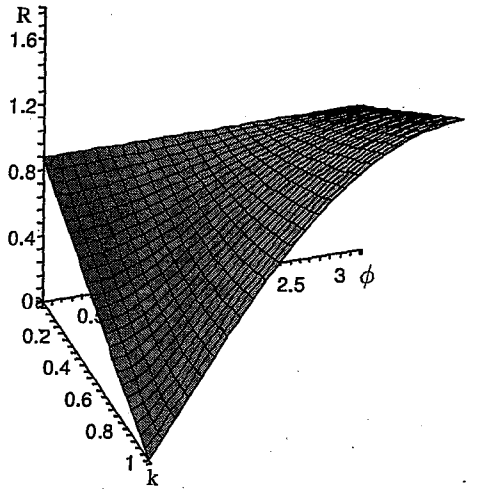

(a) R vs k and ϕ

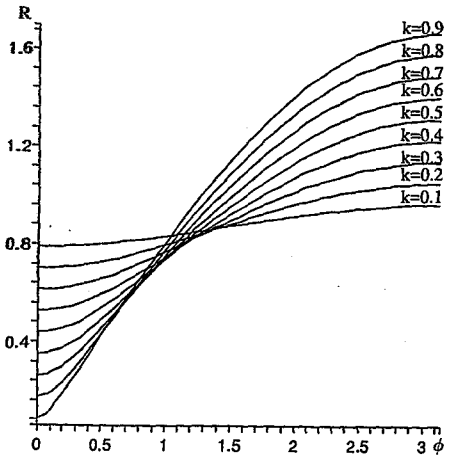

(b) R vs ϕ for given k.

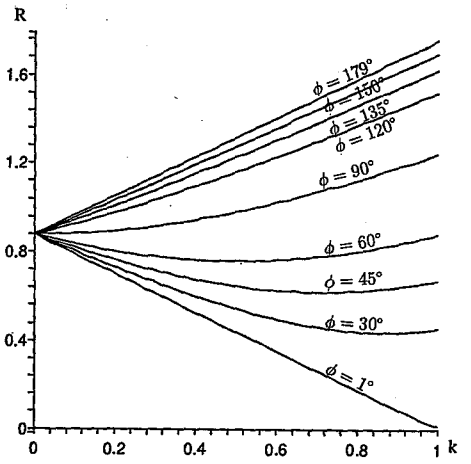

(c) R vs k for given ϕ.

Figure 2: Evolution of R vs k and ϕ ($t_1 = 2/\sqrt[4]{3}$, $t_2 = 1/\sqrt[4]{3}$, $t_3 = \sqrt[4]{3}$).

3 SINGULARITY-FREE WORKSPACE

Referring to [12], the workspace equations of 3-*RPR* parallel mechanisms can be obtained by expanding eq.(5) for three legs as follows:

$$\begin{cases} \rho_1^2 = [x - (x_p \cos\phi - y_p \sin\phi)]^2 + [y - (x_p \sin\phi + y_p \cos\phi)]^2 \\ \rho_2^2 = [x - (x_p \cos\phi - y_p \sin\phi - t_4 \cos\phi + t_1)]^2 + [y - (x_p \sin\phi + y_p \cos\phi - t_4 \sin\phi)]^2 \\ \rho_3^2 = [x - (x_p \cos\phi - y_p \sin\phi - t_5 \cos\phi + t_6 \sin\phi + t_2)]^2 \\ \quad\quad + [y - (x_p \sin\phi + y_p \cos\phi - t_5 \sin\phi - t_6 \cos\phi + t_3)]^2 \end{cases} \tag{11}$$

For a given orientation ϕ, these are three circle equations. These circles can be referred to as *workspace circles*, because they are used for determining the workspace. The three centres $C_i(x_{ci}, y_{ci})(i = 1, 2, 3)$ of the workspace circles are

$$\begin{cases} x_{c1} = x_p \cos\phi - y_p \sin\phi \\ y_{c1} = x_p \sin\phi + y_p \cos\phi \\ x_{c2} = x_p \cos\phi - y_p \sin\phi - t_4 \cos\phi + t_1 \\ y_{c2} = x_p \sin\phi + y_p \cos\phi - t_4 \sin\phi \\ x_{c3} = x_p \cos\phi - y_p \sin\phi - t_5 \cos\phi + t_6 \sin\phi + t_2 \\ y_{c3} = x_p \sin\phi + y_p \cos\phi - t_5 \sin\phi - t_6 \cos\phi + t_3 \end{cases} \tag{12}$$

The distances between the centre $C(x_c, y_c)$ of the singularity circle and the centres $C_i(x_{ci}, y_{ci})$ of the workspace circles are

$$d_i = \overline{CC_i} = \sqrt{(x_{ci} - x_c)^2 + (y_{ci} - y_c)^2} \qquad (i = 1, 2, 3) \tag{13}$$

Substituting eqs.(10) and (12) into eq.(13), one obtains $d_i \equiv R(i = 1, 2, 3)$. This means that for similar base and platform, the three centres of the workspace circles lie exactly on the singularity circle, as shown in Fig.3. Besides, from eq.(12), one obtains

$$\begin{cases} \overline{C_1C_2} = \overline{B_1B_2}\sqrt{k^2 - 2k\cos\phi + 1} \\ \overline{C_2C_3} = \overline{B_2B_3}\sqrt{k^2 - 2k\cos\phi + 1} \\ \overline{C_3C_1} = \overline{B_3B_1}\sqrt{k^2 - 2k\cos\phi + 1} \end{cases} \tag{14}$$

Eq.(14) shows that triangle $\triangle C_1C_2C_3$ is also similar to the base. Its area is

$$S = (k^2 - 2k\cos\phi + 1)S_b \tag{15}$$

where S_b is the area of the base triangle $\triangle B_1B_2B_3$. For a base of unit area ($S_b = 1$), S is constant for a given orientation ϕ.

To determine the singularity-free workspace, the minimal leg lengths $\rho_{i,min}(i = 1, 2, 3)$ should first be prescribed. As the minimal leg lengths depend on the physical architecture, they can be initially chosen as the same. With this assumption, the maximal leg length $\rho_{i,max}(i = 1, 2, 3)$ can be determined with the following procedure (taking Fig.3(a) as an example):

Step 1: Compute $C(x_c, y_c)$ and R using eq.(10) as well as $C_i(x_{ci}, y_{ci})(i = 1, 2, 3)$ using eq.(12). To compute C and C_i, it is necessary to provide the coordinates of the considered point P in the mobile frame. For convenience, take the centroid of the platform as the considered point P. Hence, $x_p = (t_4 + t_5)/3, y_p = t_6/3$.

Step 2: The intersections N_i and $N_i'(i = 1, 2, 3)$ of the minimal workspace circles and the singularity circle can be computed with eq.(16) as follows:

$$\begin{cases} (x - x_{ci})^2 + (y - y_{ci})^2 = \rho_{i,min}^2 \qquad (i = 1, 2, 3) \\ (x - x_c)^2 + (y - y_c)^2 = R^2 \end{cases} \tag{16}$$

Step 3: Compute $\rho_{i,max}(i = 1, 2, 3)$:

- Compute the distances between the centre C_1 and the two intersections N_3 and N_2': $\overline{C_1N_3}$ and $\overline{C_1N_2'}$. Then take the shortest of these distances (here $\overline{C_1N_3}$) as $\rho_{1,max}$ in order to avoid singularity inside the workspace.

- Compute the distances between the centre C_2 and the two intersections N_1 and N_3': $\overline{C_2N_1}$ and $\overline{C_2N_3'}$. Then take the shortest of these distances (here $\overline{C_2N_3'}$) as $\rho_{2,max}$.

- Compute the distances between the centre C_3 and the two intersections N_2 and N_1': $\overline{C_3N_2}$ and $\overline{C_3N_1'}$. Then take the shortest of these distances (here $\overline{C_3N_2}$) as $\rho_{3,max}$.

With the obtained maximal leg lengths, three maximal workspace circles respectively centred at $C_i(i = 1, 2, 3)$ are available. Fig. 3(a) shows only the parts of these circles lying inside the singularity circle, i.e., three arcs: M_1N_3, M_2N_3' and M_3N_2. Arc M_1N_3 intersects the second minimal workspace circle at M_4 and arc M_2N_3' intersects arc M_3N_2 at M_5. The hatched region formed by five arcs, $M_4N_3N_3'M_5N_2M_4$, is the singularity-free workspace for the considered case.

For general similar base and platform, the maximal leg lengths $\rho_{i,max}(i = 1, 2, 3)$ may be different from one another. Besides, Fig. 3(a) shows that the minimal length of leg 1 will be $\overline{C_1M_5}$, which is greater than its initially chosen value.

4 GEOMETRIC OPTIMIZATION

4.1 Maximal Singularity-Free Workspace

For a base of unit area , $t_3 = 2/t_1$. Substituting this equation into eq.(10), R will be a function of t_1, t_2, k and ϕ. To obtain an extremum of R, the following conditions should be satisfied:

$$\begin{cases} \partial R/\partial t_1 = 0 \\ \partial R/\partial t_2 = 0 \\ \partial R/\partial k = 0 \\ \partial R/\partial \phi = 0 \end{cases} \tag{17}$$

Unfortunately, there is no real solution for this equation set. However, for given nonzero k and $\phi \neq i\pi(i = 0, 1)$, a real solution can be obtained from the first two equations of eq.(17), i.e., $t_1 = 2/\sqrt[4]{3}, t_2 = 1/\sqrt[4]{3}$. As a result, $t_3 = \sqrt[4]{3}$. The obtained base is actually an equilateral triangle. In this case, one has

$$R = 2\sqrt{(k^2 - 2k\cos\phi + 1)/\sqrt{3}} \simeq 0.877\sqrt{k^2 - 2k\cos\phi + 1} \tag{18}$$

Hence, for given k and ϕ, eq.(18) provides the extreme radius of the singularity circle for a base of unit area which is obtained when the base and the platform are equilateral triangles. Since triangle $\triangle C_1C_2C_3$ is similar to the base triangle $\triangle B_1B_2B_3$, then triangle $\triangle C_1C_2C_3$ is also equilateral. As a result, the three centres $C_i(i = 1, 2, 3)$ of the workspace circles are evenly distributed on the singularity circle, as shown in Fig 3(b). In this case, both $\rho_{i,min}$ and $\rho_{i,max}$ are equal for $i = 1, 2, 3$, and the obtained singularity-free workspace (the hatched region) occupies most of the region inside the singularity circle.

However, the extreme radius given by eq.(18) for given k and ϕ is not a maximum, but a minimum. From eq.(15), it can be seen that for given k and ϕ, triangle $\triangle C_1C_2C_3$ has the same area, no matter what its shape is. And the singularity circle is the circumscribed circle of triangle $\triangle C_1C_2C_3$. When triangle $\triangle C_1C_2C_3$ is equilateral, its circumscribed circle becomes minimal. Although the minimal singularity circle occurs when the base and the platform are equilateral triangles, the singularity-free workspace may be maximal. To demonstrate this point, consider the following three case studies.

Case 1: In Fig.3(a), the base geometric parameters are: $t_1 = 1.8$, $t_2 = 1.2$, $t_3 = 1.11$, which form an acute triangle of unit area. Substituting the values of t_1, t_2 and t_3 into eq.(10), one obtains

$$R = 0.929\sqrt{k^2 - 2k\cos\phi + 1} \tag{19}$$

Case 2: In Fig.3(b), the base geometric parameters are: $t_1 = 2/\sqrt[4]{3}$, $t_2 = 1/\sqrt[4]{3}$, $t_3 = \sqrt[4]{3}$, which form an equilateral triangle of unit area. The radius of the singularity circle is given by eq.(18).

Case 3: In Fig.3(c), the base geometric parameters are: $t_1 = 1.8$, $t_2 = 2.2$, $t_3 = 1.11$, which form an obtuse triangle of unit area. Substitute the values of t_1, t_2, t_3, into eq.(10), one obtains

$$R = 1.310\sqrt{k^2 - 2k\cos\phi + 1} \tag{20}$$

Comparing eq.(18) to eq.(19) and eq.(20), it is easy to find that when the base and platform are equilateral triangles, the singularity circle is minimal. To compare the singularity-free workspace in these three cases, consider for instance the situation with $k = 0.6$, $\phi = 45°$, and $\rho_{i,min}$ is initially chosen as 0.2. First, compare case 1 to case 2. The radius of the singularity circle in case 1 is 0.665, which is larger than that (0.627) in case 2. But the area of the singularity-free workspace in case 1 is only 0.729, which is smaller than that (0.918) in case 2. Then, compare case 3 to case 2. Although the radius of the singularity circle in case 3 is 1.494 times of that in case 2, the singularity-free workspace occupies no more than one-third of the region inside the singularity circle (see Fig.3(c)). The numerical results show that the area of the singularity-free workspace in case 3 is only 0.545, which is smaller than that (0.918) in case 2.

The reason for which a robot with a larger singularity circle has a smaller singularity-free workspace is that the centres of the workspace circles , $C_i (i = 1, 2, 3)$, are not evenly distributed on the singularity circle. For given k and ϕ, the area of triangle $\triangle C_1C_2C_3$ does not vary with its shape. It is easy to imagine that for case 3 with an obtuse triangle base, when the obtuse angle becomes larger, the vertexes of the triangle $\triangle C_1C_2C_3$ will lie on an arc close to a line. Although the singularity circle may be very large, the singularity-free workspace occupies only a small corner of the singularity circle (see Fig.3(c)).

4.2 Location of the Singularity Circle

Eq.(10) shows that the centre of the singularity circle is dependent on the position of the considered point P and the orientation angle ϕ. Take the centroid of the platform as the considered point P, the centre of the singularity circle for case 1 in Fig.3(a) and case 3 in Fig.3(c) is dependent on the orientation angle ϕ, as shown in Figs. 4(a) and 4(c). In these two cases, the locus of the centre

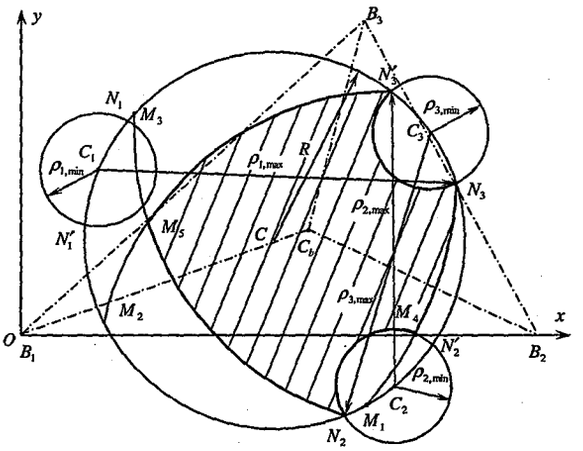

(a) Acute triangle base

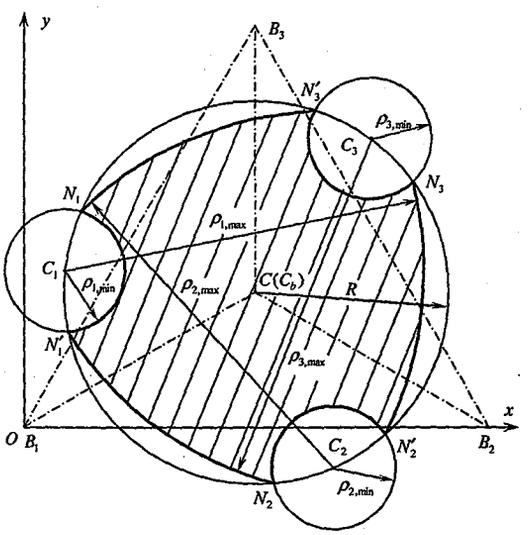

(b) Equilateral triangle base

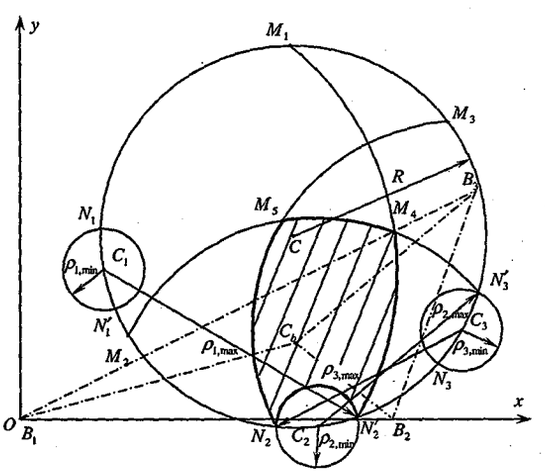

(c) Obtuse triangle base

Figure 3: The singularity-free workspace with different triangle bases.

of the singularity circle is a curve in the $xy\phi$ space. However, the centre of the singularity circle for case 2 in Fig.3(b) always coincides with the centroid of the base C_b. As a result, the locus of the centre of the singularity circle is a straight line in the $xy\phi$ space, as shown in Fig.4(b). With this property as well as the symmetry, the parallel mechanism with an equilateral triangle base will have better kinematic properties comparing to other architectures.

From the analysis of the maximal singularity-free workspace as well as the location of the singularity circle, it can be seen that a planar 3-$\underline{R}PR$ parallel mechanism with an equilateral triangle base is the optimal architecture.

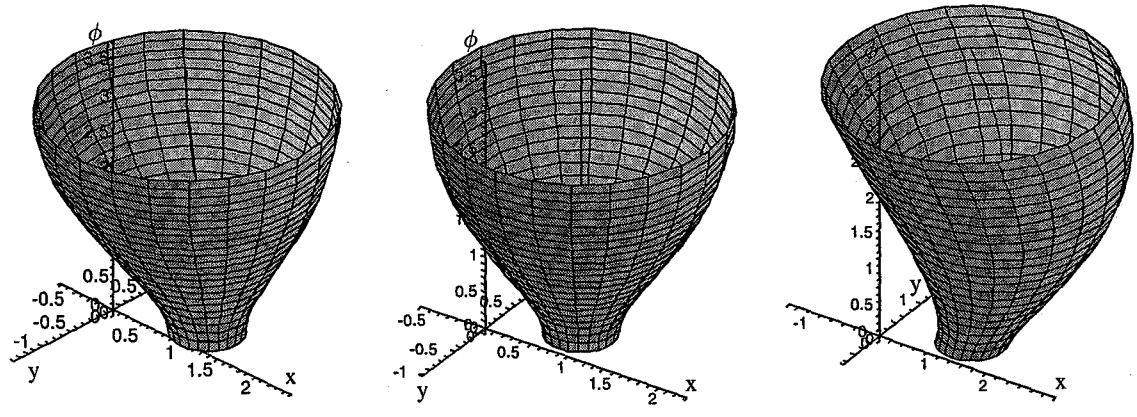

(a) Acute triangle base (b) Equilateral triangle base (c) Obtuse triangle base

Figure 4: Evolution of the singularity circle vs ϕ ($k = 0.6$).

5 APPLICATION

5.1 Design Procedure

In general, after a robot has been designed and manufactured, the size ratio k cannot change. But the orientation angle ϕ should cover a working range. Considering this point, the design procedure for 3-*RPR* robots with equilateral triangle base and platform can be generalized as follows:

- Referring to Fig.2(a) and considering the physical architecture, select a proper size ratio k.
- According to the desired function, determine a range of the orientation angle: $[\phi_1, \phi_2]$. Note that $\phi = i\pi (i = 0, 1)$ should not be included in the prescribed range.
- Referring to Fig.2(a) or Fig.2(b), use eq.(18) to compute the corresponding range of the radius of the singularity circle: $[R_1(\phi_1), R_2(\phi_2)]$.
- Considering the physical architecture such as the size of one prismatic joint and two revolute joints on one leg, determine the minimal leg lengths $\rho_{i,min} (i = 1, 2, 3)$.
- Referring to Fig.3, take the centroid of the platform as the considered point, use the procedure presented in Section 3 to compute the maximal leg lengths $\rho_{i,max} (i = 1, 2, 3)$ in order to determine the maximal leg length ranges.
- Choose a proper leg length range within the computed maximal leg length range for each leg and complete the geometric design.

5.2 Example

To demonstrate the proposed design procedure, an example is now provided. The parameters of the base are $t_1 = 2/\sqrt[4]{3}$, $t_2 = 1/\sqrt[4]{3}$, $t_3 = \sqrt[4]{3}$. The size ratio k is selected as 0.6 and the desired orientation range of ϕ is $[100°, 165°]$. Taking the minimal leg lengths as 0.2. Then $\rho_{i,max} (i = 1, 2, 3)$

is determined by $R_1(= 1.099)$ as 1.995. The possible maximal leg length range is $[0.2, 1.995]$ for all three legs. Hence, the leg length ranges can be chosen from this computed maximal leg length range, say $[0.4, 1.8]$. It can be guaranteed that no singularity exists inside the workspace of the designed robot for the prescribed range of orientation.

6 CONCLUSIONS

The derived singularity equation shows that the singularity locus of any point on the platform is a circle of the same size, as long as the base and the platform are similar triangles. Furthermore, the three centres $C_i(i = 1, 2, 3)$ of the workspace circles lie exactly on the singularity circle. These interesting observations are very useful for the determination of the singularity-free workspace. For an equilateral triangle base, $C_i(i = 1, 2, 3)$ are evenly distributed on the singularity circle which leads to the maximal singularity-free workspace.

Besides, symmetric architectures are widely used in practice. Hence, a geometric design procedure for 3-$R\underline{P}R$ robots with equilateral triangle base and platform is provided. The example discussed above shows that as long as the working ranges of the leg length lie within the maximal ranges determined with the presented method and the orientation angle ϕ does not equal $i\pi(i = 0, 1)$, it can be guaranteed that the workspace definitely lies inside the singularity circle. The risk for encountering a singularity inside the workspace can be avoided completely. Therefore, the information provided in this work will be of great significance for robot designers in practice.

Acknowledgements

The authors would like to acknowledge the financial support of the Natural Sciences and Engineering Research Council of Canada (NSERC) as well as the Canada Research Chair (CRC) Program.

REFERENCES

[1] Merlet, J.P., 1994, "Trajectory Verification In The Workspace For Parallel Manipulator", *International Journal of Robotics Research*, vol.13, No.4, pp.326–333.

[2] Bhattacharya, S., Hatwal, H., and Ghosh A., 1998, "Comparison Of An Exact And An Approximate Method Of Singularity Avoidance In Platform Type Parallel Manipulators", *Mechanism and Machine Theory*, Vol.33, No.7, pp.965–974.

[3] Dash, A.K., Chen, I.M., Yeo, S.H., and Yang G., 2003, "Singularity-Free Path Planning Of Parallel Manipulators Using Clustering Algorithm And Line Geometry", *ICRA-2003.*

[4] Gosselin, C., and Angeles, J., 1990, "Singularity Analysis Of Closed-Loop Kinematic Chains", *IEEE Transactions on Robotics and Automation*, Vol.6, No.3, pp.281–290.

[5] Ma, O., and Angeles, J., 1991, "Architecture Singularities Of Platform Manipulator", *IEEE Int. Conf. on Robotics and Automation*, Sacramento, California, USA, pp.1542–1547.

[6] Zlatanov, D., Bonev, I.A., and Gosselin, C., 2002, "Constraint Singularities Of Parallel Mech-

anisms", *Proceedings of the 2002 IEEE International Conference on Robotics and Automation*, Washington, DC, USA, pp.496-502.

[7] Zlatanov, D., Fenton, R.G., and Behhabid, B., 1994, "Singularity Analysis Of Mechanisms And Robots Via A Velocity-Equation Model Of The Instantaneous Kinematics", *Proceedings of the IEEE International Conference on Robotics and Automation*, San Diego, CA, USA, pp.986-991.

[8] Gosselin, C., and Angeles, J., 1988, "The Optimum Kinematic Design Of A Planar Three-Degree-Of-Freedom Parallel Manipulator", *Journal of Mechanisms, Transmissions, and Automation in Design*, Vol.110, pp.35–41.

[9] Sefrioui, J., and Gosselin, C., 1993, "Singularity Analysis And Representation Of Planar Parallel Manipulators", *Journal of Robotics and Autonomous System*, Vol.10, pp.209–224.

[10] Sefrioui, J., and Gosselin, C., 1995, "On The Quadratic Nature Of The Singularity Curves Of Planar Three-Degree-Of-Freedom Parallel Manipulators", *Mechanism and Machine Theory*, Vol.30, No.4, pp.533–551.

[11] Kong, X., and Gosselin, C., 2000, "Determination Of The Uniqueness Domains Of 3-*RPR* Planar Parallel Manipulators With Similar Platforms", *Proceedings of ASME 2000 Design Engineering Technical Conferences and Computers and Information in Engineering Conference*, Baltimore, Maryland, September 10-13.

[12] Gosselin, C., and Jean, M., 1996, "Determination Of The Workspace Of Planar Parallel Manipulators With Joint Limits", *Robotics and Autonomous Systems*, Vol.17, pp.129–138.

[13] Merlet, J.P., 1996, "Direct Kinematics Of Planar Parallel Manipulators", *Proceedings of the IEEE International Conference on Robotics and Automation*, April 22-28, pp.3744–3749.

[14] Daniali H.R.M., Zsombor-Murray P.J., and Angeles J., 1995, "Singularity Analysis Of Planar Parallel Manipulators", *Mechanism and Machine Theory*, Vol.30, No.5, pp.665–678.

[15] Liu, X.J., Wang, J., and Gao, F., 2000, "Performance Of The Workspace For Planar 3-DOF Parallel Manipulators", *Robotica*, Vol.18, pp.563–568.

[16] Gallant, M., and Boudreau, R., 2002, "The Synthesis Of Planar Parallel Manipulators With Prismatic Joints For An Optimal, Singularity-Free Workspace", *Journal of Robotics Systems*, Vol.19, No.1, pp.13–24.

[17] Collins C.L., and McCarthy, J.M., 1998, "The Quartic Singularity Surfaces Of Planar Platforms In The Clifford Algebra Of The Projective Plane", *Mechanism and Machine Theory*, Vol.33, No.7, pp.931–944.

[18] Arsenault, M., and Boudreau, R., 2006, "Synthesis Of Planar Parallel Mechanisms While Considering Workspace, Dexterity, Stiffness And Singularity Avoidance", *ASME Journal of Mechanical Design*, Vol.128, No.1, pp.69–78.